

# Ray-wave correspondence in limaçon-shaped semiconductor microcavities

Susumu Shinohara,<sup>1</sup> Martina Hentschel,<sup>1</sup> Jan Wiersig,<sup>2</sup> Takahiko Sasaki,<sup>3</sup> and Takahisa Harayama<sup>4</sup>

<sup>1</sup>*Max-Planck-Institut für Physik Komplexer Systeme,  
Nöthnitzer Straße 38, D-01187 Dresden, Germany*

<sup>2</sup>*Institut für Theoretische Physik, Universität Magdeburg, Postfach 4120, D-39016 Magdeburg, Germany*

<sup>3</sup>*Center for Nano Materials and Technology, Japan Advanced Institute of  
Science and Technology, 1-1 Asahidai, Nomi, Ishikawa 923-1292, Japan*

<sup>4</sup>*NTT Communication Science Laboratories, NTT Corporation,  
2-4 Hikaridai, Seika-cho, Soraku-gun, Kyoto 619-0237, Japan*

The limaçon-shaped semiconductor microcavity is a ray-chaotic cavity sustaining low-loss modes with mostly unidirectional emission patterns. Investigating these modes systematically, we show that the modes correspond to ray description collectively, rather than individually. In addition, we present experimental data on multimode lasing emission patterns that show high unidirectionality and closely agree with the ray description. The origin of this agreement is well explained by the collective correspondence mechanism.

PACS numbers: 42.55.Sa, 05.45.Mt, 42.55.Px

Strong light confinement by whispering-gallery modes of microcavities has attracted intense attention because of their potential applications in the field of lasers and photonics [1]. Conventionally, the whispering-gallery modes are realized by rotationally symmetric cavities such as disks [2] and spheres [3]. When applying these for laser cavities, however, one encounters two undesired properties: low output power and the lack of emission directionality, which are intrinsic to rotationally symmetric cavities. In order to resolve this problem, the idea of smoothly deforming a cavity shape to a rotationally asymmetric one has been proposed [4, 5], which enables the existence of high quality factor modes with highly anisotropic emissions. Nöckel et al. studied general influences of asymmetry on resonant mode characteristics such as quality factors and emission patterns in terms of the ray and wave chaos theory, revealing that microcavities offer a good stage for the concepts and techniques of the classical and quantum chaos theory to play an essential role [4]. Since then, optical microcavities with various shapes have been studied both theoretically and experimentally, with the motivation to control light emission by a cavity shape and/or to understand the effect of ray chaos on the cavity's wave characteristics [6, 7, 8, 9, 10, 11, 12, 13, 14, 15, 16, 17].

One of the goals of using the cavity shape to control light emission is the achievement of highly unidirectional microlasers. Recently, on the basis of the ray and wave chaos theory, it has been predicted that a semiconductor microcavity with a shape called the limaçon of Pascal exhibits a highly unidirectional lasing emission pattern, while maintaining relatively high quality factors [18]. The limaçon shape is defined, in the polar coordinates  $(\rho, \phi)$ , by  $\rho(\phi) = R(1 + \epsilon \cos \phi)$ , where  $R$  and  $\epsilon$  are size and deformation parameters, respectively. The cavity shape is shown in the inset of Fig. 1 (a). For  $\epsilon$  values around 0.43, the ray dynamics inside the cavity becomes predominantly chaotic. The ray chaos results in a highly unidirectional emission, when the re-

fractive index  $n$  is chosen around 3.3. In Ref. [18], it is reported that every low-loss resonant mode exhibits a similar, or universal emission pattern corresponding to a ray-calculated pattern, which is attributed to the ray-dynamical emission mechanism governed by unstable manifolds [13]. This analysis of resonant modes was carried out for the dimensionless size parameter  $nkR \approx 86$ , where  $k$  is the free-space wave number. Because low-loss modes, which are most likely to be excited in lasing experiments, have similar highly unidirectional emission patterns, laser light output to a single direction is expected with this cavity shape. This robust mechanism for the appearance of unidirectional lasing emission differentiates the limaçon shape from the other shapes previously proposed to achieve unidirectionality [9, 10, 19]. Motivated by such an attractive feature, Song et al. and Yan et al. have fabricated limaçon-shaped semiconductor microcavities independently [20, 21]. Although they both succeeded in observing mostly unidirectional outputs, detailed correspondence between experimental and ray-calculated emission patterns has not been studied. It is one of the aims of this paper to study such correspondence.

In this paper, we study theoretically and experimentally the limaçon-shaped semiconductor microcavities larger than those previously studied. For larger cavities, better correspondence between experiment and ray-calculation is expected, since ray description is generally expected to work better in a shorter wavelength regime. We theoretically investigate resonant modes for  $nkR \approx 484$  and perform experiments for fabricated limaçon-shaped single-quantum-well laser diodes with  $nkR \approx 484$  and  $nkR \approx 1210$ . These sizes are much larger than the cavities of Song et al. ( $nkR \approx 48$ ) and those of Yan et al. ( $nkR \approx 161$ ). In the theoretical analysis, we point out a phenomenon revealed only for larger  $nkR$ , that is, mode-dependent discrepancies of individual modes' emission patterns from the ray-calculated pattern, which is contrasted with the observation of the universal pat-

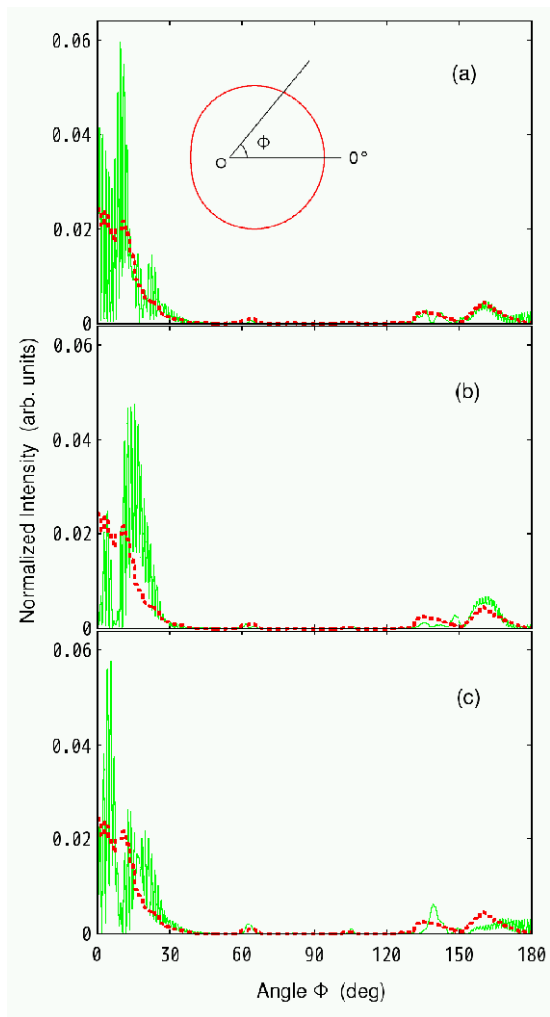


FIG. 1: (Color online) Far-field emission patterns of the limaçon-shaped microcavities. The solid curves are for the three lowest-loss resonant modes with odd parity: (a)  $RenkR = 484.11$ ,  $ImnkR = -0.0017$ ; (b)  $RenkR = 483.84$ ,  $ImnkR = -0.0017$ ; (c)  $RenkR = 484.75$ ,  $ImnkR = -0.0024$ . The dotted curve is a ray-calculated pattern. The far-field angle  $\phi$  is defined in the inset of (a). Because the patterns are symmetric with respect to the  $\phi = 0$  axis, only the half angular range is shown.

tern for smaller  $nkR$  [16, 18]. In spite of such discrepancies, we demonstrate that ray-wave correspondence can be recovered by averaging emission patterns of many low-loss modes. This averaged pattern can be considered as the approximate of a multimode lasing emission pattern. In experiments, we observe highly unidirectional lasing emission patterns, which closely correspond to the ray-calculated pattern even for smaller subpeaks.

First, we report theoretical results of resonant modes for  $nkR \approx 484$ . Taking into account that experimentally observed light is transverse electric (TE) polarized, we calculated resonant modes for the TE polarization by using the boundary element method [22]. In Fig. 1, we plot far-field patterns of low-loss modes together with

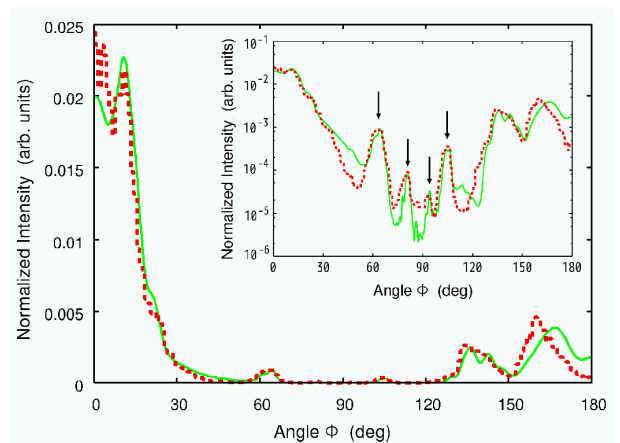


FIG. 2: (Color online) The average of the far-field emission patterns for the 42 lowest-loss modes (solid curve) and the ray-calculated pattern (dotted curve). The inset shows the semi-log plot of these patterns.

the ray-calculated result. We found 112 low-loss modes in the range  $483.8 < nkR < 485.4$ . The modes shown in Fig. 1 are the three lowest-loss odd-parity modes. The far-field patterns are normalized so that integration becomes unity. Each of these far-field patterns shows correspondence with the ray-calculated pattern to some extent. However, closer inspection reveals mode-dependent slight deviations from the ray-calculated result that do not vanish even when rapid oscillations are smeared out. Such deviations have been observed also for resonant modes of the stadium-shaped cavities with  $nkR \approx 330$  [23, 24]. These results suggest that, in general, the emission pattern of an individual mode does not converge to a ray-calculated pattern in the short-wavelength limit, even after wave interference effects are smeared out. On the contrary, in smaller  $nkR$  cases, an individual mode lacks enough resolution to manifest its deviation from the ray-calculated pattern, which appears to be a reason less attention was paid for the deviations of individual modes from the ray calculation in the previous works on smaller  $nkR$  cases.

Next, we demonstrate that the deviations of individual modes are averaged out, if the far-field patterns are averaged over many low-loss modes. In Fig. 2, we show the averaged far-field pattern for 42 lowest-loss modes, where one can observe improved agreement between the wave and ray calculations. Although there is an arbitrariness on how we put a weight to each mode when taking the average, here we put an equal weight. Starting from a single mode, we checked that the agreement improves by increasing the number of averaged modes  $N$ , and a converged pattern is obtained for  $N \approx 42$ . Notably, even tiny peaks at around  $\phi = 63, 80, 93, 104$  degrees of the ray-calculated pattern can be reproduced in the averaged wave-calculated pattern, which is clearly seen in the semi-log plot shown in the inset of Fig. 2, where the four peaks are indicated by arrows. The convergence

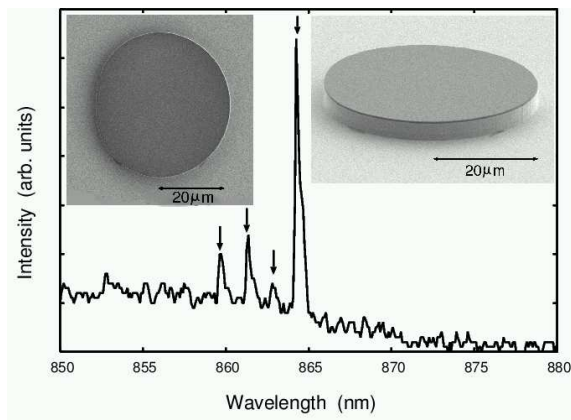


FIG. 3: (Color online) Lasing spectrum for the limaçon-shaped single-quantum-well laser diodes with  $\epsilon = 0.43$  and  $R = 20 \mu\text{m}$ . The pumping current is 25 mA, which is slightly above the lasing threshold. Insets: Scanning electron microscope images of the limaçon-shaped semiconductor microcavity with  $\epsilon = 0.43$  and  $R = 20 \mu\text{m}$  before a contact layer is fabricated on the top: Top view (left inset) and oblique view (right inset).

to ray calculation in the limaçon-shaped cavity is better than that in the stadium-shaped cavity [23, 24]. We expect this difference can be explained by the fact that the overlap of the Fresnel weighted unstable manifold with a leaky phase space area for the limaçon-shaped cavity [18] is much smaller than that for the stadium-shaped cavity [23], whose detailed discussion will be presented elsewhere.

Concerning the rightmost peak at around  $\phi=165$  degrees, one can recognize a slight peak shift between the ray-calculated and wave-calculated patterns. By analyzing the ray dynamics, we found that, among all the tiny peaks, only the rightmost peak is formed from rays refracted by the cavity boundary with the incident angle close to the critical angle for total internal reflection. It is known that emission close to total internal reflection can be largely affected by the Goos-Hänchen effect and the Fresnel filtering effect [25, 26], causing discrepancies between ray and wave calculations, although these effects are supposed to vanish in the short-wavelength limit. A detailed analysis is now in progress to identify the cause of the peak shift, which will be reported elsewhere.

The above averaged pattern is not just an artificial product, but has a physical meaning that it approximates a multimode lasing emission pattern. In order to study multimode lasing phenomena, one has to take into account nonlinear interaction among modes caused by a lasing medium, as has been done in Refs. [27, 28]. Generally, there is no convenient method to predict properties of a multimode lasing state from those of the (passive) modes involved in lasing. However, the averaged far-field pattern of low-loss modes with equal weights can be considered as the time-averaged far-field pattern of a multimode lasing state, provided that the gain band of a

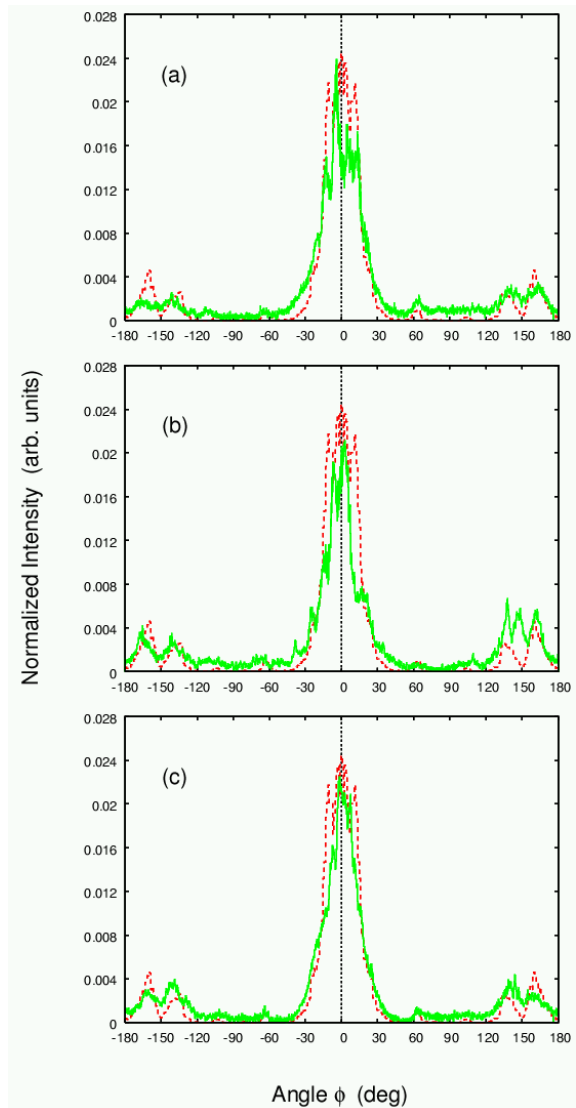


FIG. 4: (Color online) Far-field emission patterns of the limaçon-shaped single-quantum-well laser diodes (solid curves) and the ray-calculated pattern (dotted curves). (a) and (b) are for two different samples with  $R = 20 \mu\text{m}$ , which are fabricated from the same epiwafer. (c) is for a cavity with  $R = 50 \mu\text{m}$ . The deformation parameter  $\epsilon$  is 0.43 in all the cavities.

lasing medium is so broad compared to an averaged mode spacing that many modes are equally excited, and mode couplings are not so strong that a multimode lasing state is dynamically described by a high dimensional torus. If these assumptions are satisfied, one can expect that a multimode lasing state is approximated by the averaged low-loss modes, thus exhibiting an emission pattern closely corresponding to a ray-calculated pattern. Below, we examine this correspondence in the experiment of the limaçon-shaped single-quantum-well laser diodes.

We fabricated limaçon-shaped microcavities with  $\epsilon = 0.43$  for  $R = 20 \mu\text{m}$  (i.e.,  $nkR \approx 484$ ) and  $R = 50 \mu\text{m}$  (i.e.,  $nkR \approx 1210$ ). We note that the above

wave calculations are directly applicable for the fabricated cavities with  $R = 20 \mu\text{m}$ . In the fabrication, we used a metal-organic chemical vapor deposition grown gradient-index, separate-confinement-heterostructure, single-quantum-well GaAs/Al<sub>x</sub>Ga<sub>1-x</sub>As structure. The cavity geometry was defined by electron beam lithography and a reactive ion etching technique. The details of the structure and fabrication process are precisely the same as those in Ref. [12]. The effective refractive index of our microcavities is  $n = 3.3$ , which is estimated from the single-quantum-well epiwafer structure. The insets of Fig. 3 show the scanning electron microscope images of the limaçon-shaped microcavity with  $R = 20 \mu\text{m}$ , where one can confirm the high degree of smoothness and verticality of the cavity boundary. Lasing experiments are carried out at room temperature and with electrical pumping. A pulsed current has 500-ns width at a 1 kHz repetition. The lasing threshold is estimated as 22 mA for  $R = 20 \mu\text{m}$  and 34 mA for  $R = 50 \mu\text{m}$ . The lasing phenomenon was confirmed by the appearance of narrow peaks in the spectrum, where the peaks are observed around 865 nm. In Fig. 3, we plot lasing spectrum for the cavity with  $R = 20 \mu\text{m}$  and pumping current 25 mA, which is slightly above the lasing threshold. The mode spacing of the four peaks in Fig. 3 is 1.7 nm, which corresponds to the optical path-length of the circumference, i.e.  $\Delta\lambda \approx \lambda^2/(2\pi nR) = 1.8$  nm. By increasing the pumping current, many modes are involved in lasing. Although we could not resolve individual lasing modes because of the resolution limit of our spectrometer, from the estimate of the averaged mode spacing, we expect that at least 40 modes are involved for the cavity with  $R = 20 \mu\text{m}$  at the current 200

mA.

Figure 4 (a)-(c) show measured far-field patterns (solid curves) with the ray-calculated pattern (broken curves). Figures 4 (a) and 4 (b) are for two different cavities with  $R = 20 \mu\text{m}$ , which are fabricated from the same epiwafer, and Fig. 4 (c) is for a cavity with  $R = 50 \mu\text{m}$ . The pumping current is 200 mA for all the data in Fig. 4. These experimental far-field patterns show close correspondence with the ray-calculated patterns. Remarkably, one can see correspondence even for smaller peaks at 136 and 160 degrees to some extent. We checked that for sufficiently large pumping, such good correspondence is observed robustly.

In summary, for the limaçon-shaped semiconductor microcavities, we have shown that low-loss resonant modes exhibit mostly unidirectional emission patterns, but there are mode-dependent slight discrepancies from the ray-calculated pattern. Nonetheless, we demonstrated that an averaged emission pattern of many low-loss modes, which can be regarded as the approximate of a multimode lasing emission pattern, closely corresponds to the ray-calculated pattern. In addition, we present experimental far-field data, which provide convincing evidence not only of highly unidirectional lasing emission but of the capability of the ray calculation to reproduce experimental multimode lasing emission patterns. We expect the results presented here can be applied to other cavities having predominantly chaotic ray dynamics.

We would like to thank J.-W. Ryu and J. Unterhinninghofen for discussions. S.S., M.H. and J.W. acknowledge financial support from the DFG research group 760 ‘‘Scattering Systems with Complex Dynamics’’ and the DFG Emmy Noether Program.

- 
- [1] K. J. Vahala, *Nature* **424**, 839 (2003).  
 [2] S. L. McCall *et al.*, *Appl. Phys. Lett.* **60**, 289 (1992).  
 [3] L. Collot *et al.*, *Europhys. Lett.* **23**, 327 (1993).  
 [4] J. U. Nöckel *et al.*, *Opt. Lett.* **19**, 1693 (1994); J. U. Nöckel *et al.*, *Opt. Lett.* **21**, 1609 (1996); J. U. Nöckel and A. D. Stone, *Nature* **385**, 45 (1997); J. U. Nöckel and A. D. Stone, in *Optical Processes in Microcavities*, R. K. Chang and A. J. Campillo, eds. (World Scientific, Singapore, 1996).  
 [5] C. Gmachl *et al.*, *Science* **280**, 1556 (1998).  
 [6] S.-B. Lee *et al.*, *Phys. Rev. Lett.* **88**, 033903 (2002).  
 [7] M. Hentschel and K. Richter, *Phys. Rev. E* **66**, 056207 (2002).  
 [8] J. Wiersig, *Phys. Rev. A* **67**, 023807 (2003).  
 [9] G. D. Chern *et al.*, *Appl. Phys. Lett.* **83**, 1710 (2003).  
 [10] M. S. Kurdoglyan *et al.*, *Opt. Lett.* **29**, 2758 (2004).  
 [11] Y. Baryshnikov *et al.*, *Phys. Rev. Lett.* **93**, 133902 (2004).  
 [12] T. Fukushima and T. Harayama, *IEEE Sel. Top. Quantum Electron.* **10**, 1039 (2004).  
 [13] H. G. L. Schwefel *et al.*, *J. Opt. Soc. Am. B* **21**, 923 (2004).  
 [14] W. Fang *et al.*, *Opt. Express* **13**, 5641 (2005).  
 [15] M. Lebental *et al.*, *Appl. Phys. Lett.* **88**, 031108 (2006).  
 [16] S.-B. Lee *et al.*, *Phys. Rev. A* **75**, 011802(R) (2007).  
 [17] T. Tanaka *et al.*, *Phys. Rev. Lett.* **98**, 033902 (2007).  
 [18] J. Wiersig and M. Hentschel, *Phys. Rev. Lett.* **100**, 033901 (2008).  
 [19] J. Wiersig and M. Hentschel, *Phys. Rev. A* **73**, 031802(R) (2006).  
 [20] Q. Song *et al.*, arXiv:0810.3923v1.  
 [21] C. Yan *et al.*, *Appl. Phys. Lett.* **94**, 251101 (2009).  
 [22] J. Wiersig, *J. Opt. A: Pure Appl. Opt.* **5**, 53 (2003).  
 [23] S. Shinohara *et al.*, *Phys. Rev. A* **77**, 033807 (2008).  
 [24] M. Choi *et al.*, *Opt. Exp.* **16**, 17554 (2008).  
 [25] F. Goos and H. Hänchen, *Ann. Phys. (Leipzig)* **436**, 333 (1947); M. Hentschel and H. Schomerus, *Phys. Rev. E* **65**, 045603(R) (2002); H. Schomerus and M. Hentschel, *Phys. Rev. Lett.* **96**, 243903 (2006); J. Unterhinninghofen *et al.*, *Phys. Rev. E* **78**, 016201 (2008).  
 [26] H. E. Tureci and A. D. Stone, *Opt. Lett.* **27**, 7 (2002).  
 [27] T. Harayama *et al.*, *Phys. Rev. Lett.* **90**, 063901 (2003); T. Harayama *et al.*, *Phys. Rev. A* **72**, 013803 (2005); S. Sunada *et al.*, *Phys. Rev. E* **71**, 046209 (2005).  
 [28] H. E. Tureci *et al.*, *Phys. Rev. A* **76**, 013813 (2007); H. E. Tureci *et al.*, *Science* **320**, 643 (2008).